Current Research in Food Science 10 (2025) 100965

Contents lists available at ScienceDirect

Current Research in Food Science

journal homepage: www.sciencedirect.com/journal/current-research-in-food-science

Exploring the effect of natural deep eutectic solvents on zein: Structural and functional properties

Adieh Anvar [a], Mohammad Hossein Azizi [a,**], Hassan Ahmadi Gavlighi [a,b,*]

[a] Department of Food Science and Technology, Faculty of Agriculture, Tarbiat Modares University, Tehran, Iran
[b] Halal Research Center of IRI, Iran Food and Drug Administration, Ministry of Health and Medical Education, Tehran, Iran

ARTICLE INFO

Handling Editor: Professor Aiqian Ye

Keywords:
Deep eutectic solvent
Functional properties
Protein modification
Zein

ABSTRACT

This study evaluated the effects of chemical modification, including ethanol, acetic acid, and natural deep eutectic solvents (NADES), on the secondary and tertiary structures, hydrophobicity, free amine content, protein-protein interactions, and functional properties of zein. The NADES used included choline chloride: oxalic acid, choline chloride: urea, choline chloride: glycerol, and glucose: citric acid. The results reveal that the NADES system significantly altered zein's structures, as evidenced by Fourier transform infrared spectroscopy, fluorescence, and Ultraviolet–Visible Spectroscopy analysis. Circular dichroism spectroscopy analysis indicated significant conformational change in modified zein, with decreased α-helix and increased random coil content. Notably, the NADES system leads to greater disruption of hydrogen bonds and facilitates the exposure of hydrophobic regions compared to water, ethanol, and acetic acid systems. This resulted in enhanced solubility, surface hydrophobicity, and free amine content in zein, indicating a more significant change in protein structure. In contrast, water and acetic acid solvents maintained more stable disulfide bonds within zein, which correlates with lower solubility and less unfolding. The NADES system promoted interactions between zein and its solvent components, improving emulsifying properties. Water, ethanol, and acetic acid systems had higher solubility in urea, thiourea, and dithiothreitol than the NADES system, revealing disruption of both covalent and noncovalent bonds in zein modified by NADES. Overall, this study highlights the superior ability of the NADES system to modify zein's structure and functionality compared to conventional solvents, suggesting its potential for enhancing protein applications in the industrial production of foods.

1. Introduction

Zein, a predominant protein in corn gluten meal, comprises 50–80% of the total protein content (He et al., 2021). This protein is categorized into α, β, γ, and δ fractions based on their molecular weight and structure (Dong et al., 2020). The structural model of zein reveals that over half of its solvent-accessible surface area comprises hydrophobic residues. Specifically, α-zein making up about 70% of total zein, is water-insoluble and exhibits an α-helix secondary structure (Bean et al., 2021; Qu, 2019). Zein's insolubility in water is attributed to its low content of polar-charged amino acids, resulting in a tendency for aggregation, thereby limiting the functional properties of zein. As a result, zein is primarily intended for animal consumption and is not typically used as a human food ingredient (Cabra et al., 2007). Therefore, modifying zein's structure to enhance its functional properties can expand its applications in food formulation.

Various strategies including chemical solvents, physical techniques, and enzymatic reactions have been investigated to alter proteins' structure and physicochemical characteristics. These modifications can result in proteins with more desirable functional properties than their native counterparts (Glusac and Fishman, 2021; Fu et al., 2020). Among these methods, moderate chemical treatments through partial unfolding of zein molecules can improve their functional properties (Zhang et al., 2011). These treatments can unfold the protein structure by disrupting the non-covalent forces that maintain its native structure. However, excessive modification can lead to fragmentation and truncation of the zein backbone, reducing its functionality (Cabra et al., 2007).

Organic solvents like ethanol and acetic acid are commonly used in industries and research (Shishov et al., 2022). Zein is soluble in these solvents, with partial unfolding observed in both solvents, affecting its

* Corresponding author. Department of Food Science and Technology, Faculty of Agriculture, Tarbiat Modares University, Tehran, Iran.
** Corresponding author.
E-mail addresses: azizit_m@modares.ac.ir (M.H. Azizi), Ahmadi_ha@modares.ac.ir (H.A. Gavlighi).

https://doi.org/10.1016/j.crfs.2024.100965
Received 18 July 2024; Received in revised form 15 December 2024; Accepted 19 December 2024
Available online 20 December 2024

physical, structural, and rheological properties (Mattice and Marangoni, 2020). These traditional organic solvents are toxic, dangerous, potentially explosive, highly flammable, and environmentally harmful (Negi et al., 2024). A class of innovative, environmentally friendly solvents known as natural deep eutectic solvents (NADES) has emerged to address these issues. Using chemicals generally recognized as safe (GRAS) in preparing NADES can help reduce toxicity (Yap and Gan, 2024). NADES offer a safe alternative to hazardous solvents, thus promoting a more environmentally friendly approach to green chemistry (Shishov et al., 2022). Due to their thermal stability, inexpensive, non-toxicity, low volatility, and non-flammability, NADES are attractive for various sustainable applications (Fu et al., 2020; Qu, 2019). The production of NADES is easy, and due to the variety of component combinations, their properties can be modified. NADES are mixtures of substances that function as hydrogen bond donors (HBD), including urea, polyols, organic acids, and carbohydrates, and as hydrogen bond acceptors (HBAs), like choline chloride (Yu et al., 2023a). Choline chloride is an easily accessible, cheap, biodegradable, and non-toxic quaternary ammonium salt that is a common HBA in NADES production, reacting with various HBD (Yu et al., 2023a).

NADES has been used to modify and extract various compounds in several studies. Yu et al. (2023b) used hydrophobic NADES to extract lycopene from tomato powder with high extraction yields. Qu (2019) showed that NADES could modify gelatin, zein, and soy protein to produce mechanically strong materials with a high amorphous form. Esquembre et al. (2013) reported that NADES can change the conformation of lysozyme, leading to loss of stability and the formation of intermediate states in the protein folding process. Additionally, NADES has also been used to extract proteins from sesame meal (Cao et al., 2023) and oatmeal (Yue et al., 2021), and these studies have shown that NADES can alter the structure and functionality of proteins. Cao et al. (2021) and Fu et al. (2020) used NADES as the reaction medium to modify wheat gluten and bovine serum albumin.

Until now, no study has investigated the modification of zein using NADES as a novel technique with the potential to further enhance its functional properties. Thus, the purpose of this study was to compare the structural and functional properties of zein modified with traditional solvents and NADES. To assess changes in protein structure, Fourier transform infrared (FTIR) spectroscopy, circular dichroism (CD) spectroscopy, fluorescence spectroscopy, and UV–visible spectroscopy were utilized. Furthermore, the effects of these changes on the solubility, emulsifying, foaming, and water and oil absorption capacities of zein were investigated.

2. Material and method

2.1. Materials

Corn gluten meal (CGM) with 55% protein content was obtained from Zar Ind. Co. (Tehran, Iran). choline chloride (≥98.0%), Bovine serum albumin (BSA) (96%), 2,4,6-trinitrobenzene sulfonic acid solution (TNBS) (95%) and glucose (≥99.5%), were purchased from Sigma-Aldrich (St. Louis, MO, USA), glycerin (≥99.5%), urea (≥99.5%), oxalic acid (≥99.0%), citric acid (≥98%), acetic acid (≥99%) were obtained from Merck (Darmstadt, Germany). Ammonium salt of 1-anilino-8-naphtalene-sulphonic acid (ANS) (≥90%) was obtained from Sigma-Aldrich (Vallensbaek Strand, Denmark). Other chemicals were obtained from Merck (Darmstadt, Germany).

2.2. Zein extraction from CGM

Zein was extracted from CGM following the procedure outlined by Anvar et al. (2024). CGM was immersed in a solution of 0.1 M sodium hydroxide, and 95% ethanol (45:55, v/v) for 2 h at 50 °C. The mixture underwent centrifugation. Subsequently, distilled water was added to the supernatant, and 1M HCl was used to adjust the pH to 6.3. After adding a 2% NaCl solution (1:5, v/v), the mixture was centrifuged and freeze-dried using an Alpha 2–4 LD plus freeze dryer (Christ, Germany) after being incubated for 1 h. Using Automated Kjeldahl (Foss, Kjeltec™ 8200), the Kjeldahl method calculated the crude protein content (92%) (AACC, 2000).

2.3. Modification of zein

2.3.1. Modification by ethanol, acetic acid

Modification with ethanol, acetic acid, and water was performed according to the method of Mattice and Marangoni (2020). Zein solutions were prepared in water (Z-Water), ethanol (Z-Et), and acetic acid (Z-Ac) at ratios of 6:1, 1:2, and 1:2, respectively. Following 3 h of incubation at 40 °C, the mixtures were freeze-dried. Zein, extracted from CGM, was considered a control sample.

2.3.2. Modification by NADES

Choline chloride (ChCl) and glucose (Glu) were used as HBA, while urea, oxalic acid (OA), glycerol (Gly), and citric acid (CA) were utilized as HBD, with water acting as a third component to lower their viscosity. The NADES was prepared by the method described by Shishov et al. (2022). Two components were mixed in various molar ratios (Table 1) at 80 °C by a magnetic stirrer (300 rpm) until a homogenous liquid was formed.

Using the method explained by Fu et al. (2020), the modification process with NADES was completed. Zein and these solvents were mixed in a 1:20 ratio at 200 rpm and heated to 80 °C. The mixtures were diluted to a 40% concentration and heated for 2 h at 80 °C. Finally, the samples were dialyzed for 24 h at room temperature in dialysis bags (3.5 kDa molecular weight cut-off) and freeze-dried.

2.4. Structural characterization of modified zein protein

2.4.1. Fourier-transform infrared spectroscopy (FTIR)

According to Zhang et al. (2022), KBr pellets were prepared to obtain the FTIR spectra of native and modified zein using the AVATAR 370 spectrometer (Thermo Nicolet, USA). The spectroscopic data was acquired using 32 scans with a resolution of 4 cm^{-1} in the 4000-400 cm^{-1} region.

2.4.2. CD measurement

A CD spectropolarimeter (JASCO Corporation, Tokyo, Japan) was used to measure the far-UV CD spectra of native and modified zein. The measurements were taken between 190 and 250 nm with a constant nitrogen flush and a path length of 0.1 cm. J715Standard Analysis software was then used to analyze the data. To estimate the contents of secondary structures (α-helix, β-sheet, β-turn, and random coils), Dichroweb, the online Circular Dichroism Web site (http://dichroweb.cryst.bbk.ac.uk), was used (Dai et al., 2016).

2.4.3. Tertiary structure

2.4.3.1. Intrinsic fluorescence spectra. A fluorescence spectrophotometer (LS45, PerkinElmer, Waltham, MA, USA) was used to perform fluorescence spectra following the procedure described by Fu et al. (2020). 70% ethanol was used to prepare the samples (0.2 mg/ml). Emission spectra were recorded at 250 and 500 nm at a scanning rate of 100 nm/min.

Table 1
Molar ratios of components to the preparation of NADES.

		Molar ratio
NADES	ChCl - Gly	1:2
	ChCl - OA	1:1
	ChCl - Urea	1:2
	Glu - CA	1:1

2.4.3.2. Ultraviolet–visible (UV–visible) absorbance. A UV–visible spectrophotometer (Agilent Cary 60, USA) was used to measure the UV–visible spectra of protein samples, as described by Fu et al. (2020). The samples were prepared using 70% ethanol at a concentration of 0.2 mg/ml. Each sample was scanned at 2 nm intervals between 200 and 700 nm.

2.4.4. Protein-protein interactions

The Dent et al. (2023) approach assessed both covalent and non-covalent interactions between proteins. Proteins participating in hydrogen bonding and hydrophobic interactions were isolated using a PBS solution (100 mM, pH 7.5) with the addition of either 8 M urea or 2 M thiourea. Proteins with disulfide bonds were extracted using PBS containing dithiothreitol (DTT) (50 mM). Proteins with both disulfide bonds and HBs were extracted using PBS containing urea and DTT. Protein-protein interactions were assessed using these different extraction solutions. Solubility was assessed using the Bradford method (Bradford, 1976), which included centrifugation at 13,750 g for 20 min and dilution (2–7 times).

2.4.5. Free amine group content

The He et al. (2021) method was employed to determine the samples' free amine group content. samples were freeze-dried and dissolved in deionized water (5 mg/ml). Then, 250 μL of the sample solution was combined with 1 ml of 0.01% (w/v) TNBS solution and 2 ml of 0.2 M phosphate buffer (pH 8.2). After heating at 50 °C for 30 min, 2 ml of a 0.1 M sodium sulfite solution, was added to stop the reaction. The absorbance at 420 nm was measured to determine the content of free amine groups in the samples. This determination was conducted using Equation (1), based on an L-leucine standard curve ranging from 0 to 20 mM.

$$Y = 0.2392x + 0.4902 \quad (1)$$

where Y represents the absorbance at 420 nm, and X denotes the concentration of free amine groups (mM).

2.4.6. Free sulfhydryl group and disulfide bond content

The method of Sun et al. (2020) was used to measure the free and total sulfhydryl of the protein. Free sulfhydryl was determined by dispersing freeze-dried samples in Tris-glycine buffer with 8 M urea (5 mg/ml), shaking (400 rpm) overnight at 23 °C, and centrifuging (3000 g for 10 min). Then, the supernatant was diluted and reacted with Ellman's reagent. Total sulfhydryl was determined by breaking disulfide bonds in Tris-glycine buffer (pH 8.0) containing β-mercaptoethanol (1.25% v/v), precipitating proteins with TCA (12% w/v), collecting, washing, and suspending them in Tris-glycine buffer 8 M urea. The protein solution was diluted with Tris-glycine buffer and reacted with the reagent Ellman. At 412 nm, absorbance was measured.

$$\text{Free sulfhydryl } \mu\text{mol} \Big/ \text{g} = \frac{73.53 \times (\text{A sample} - \text{A blank}) \times \text{D}}{\text{C}} \quad (2)$$

Where C represents the protein concentration (1 mg/ml) and D is the dilution factor (10 ×).

$$\text{Disulfide bond } (\mu\text{mol}/\text{g}) = \frac{\text{Total sulfhdryl} - \text{Free sulfhdryl}}{2} \quad (3)$$

2.4.7. Surface hydrophobicity (H_0)

The fluorescent probe ANS was used to measure the H_0, according to Cui et al. (2022) method. Samples (0–4.0 mg/ml) were mixed with the ANS solution in a 96-well microplate. A Cytation 3 multi-mode plate reader (BioTek Instruments, Inc., Winooski, Vermont, USA) was then used to measure the fluorescence intensity. H_0 was calculated by determining the slope of the curve depicting the relationship between fluorescence intensity and protein concentration.

2.4.8. SDS-Polyacrylamide gel Electrophoresis (SDS-PAGE)

SDS-PAGE analysis was performed using the method outlined by Fu et al. (2020) using a 15% separating gel and a 4% stacking gel. Protein samples were diluted to 2 mg/ml in phosphate buffer solution (pH 7.0) and mixed with a protein-loading dye containing β-mercaptoethanol in a 3:1 ratio. Then, the mixture was heated for 5 min at 100 °C. The samples were centrifuged at 8000 g for 5 min. Then, 10 μl of each supernatant was loaded into the corresponding wells of an SDS-PAGE gel. A standard protein marker (10–250 kDa) was also loaded. Electrophoresis was done at 120 V for 2 h for the stacking and separating gel. Finally, Coomassie Brilliant Blue R250 was used to stain the gels.

2.4.9. Functional properties

2.4.9.1. Protein solubility. Using the slightly modified He et al. (2021) method, the solubility of the samples was assessed. Sample solutions (5 mg/ml), after 30 min of stirring and adjustment to various pH levels (4, 7, and 10), were centrifuged at 6000 g for 15 min to separate the supernatant. The protein content of the supernatant was determined using the Lowry method (Lowry et al., 1951), with BSA as a standard. To prepare the prepared reagent, 50 ml of reagent A (2% sodium carbonate in 0.10 N sodium hydroxide) and 1 ml of reagent B (1.56% copper(II) sulfate in 2.37% potassium sodium tartrate) were combined. Then, two ml of the prepared reagent was mixed with 200 μl of the supernatant. The solution was then mixed with the Folin-phenol reagent, and after 30 min, the absorbance at 750 nm was measured. The solubility percentage is calculated by dividing the amount of protein in the supernatant (g) by the total amount of protein (g). This result is then multiplied by 100 to express the solubility as a percentage.

2.4.9.2. Emulsifying properties. The emulsifying properties of samples were determined using a method, as described by Zhang et al. (2022). Sample solutions (2 mg/ml) were adjusted to pH 7.0 and mixed with corn oil for 1 min at 10,000 rpm using a high-speed homogenizer (IKA-RCR-B). Absorbance at 500 nm was measured immediately and after 10 min following the combination of 50 μl of emulsion (extracted from the bottom of the container) with 5 ml of SDS solution (1 mg/ml). The emulsifying activity index (EAI) and emulsion stability index (ESI) were calculated using equations (4) and (5).

$$\text{EAI } (\text{m}^2/\text{g}) = \frac{2 \times 2.303}{\text{C} \times (1 - \phi) \times 10^4} \times \text{A0} \times \text{D} \quad (4)$$

$$\text{ESI } (\%) = \frac{\text{A10}}{\text{A0}} \times 100 \quad (5)$$

where D is the dilution factor, C is the initial protein concentration, ϕ is the volume percent of dispersed oil, and A_0 and A_{10} are the absorbance at 0 and 10 min, respectively, at 500 nm.

2.4.9.3. Foaming properties. To determine foaming capacity (FC) and foam stability (FS), the method described by Mahalaxmi et al. (2022) was used. 20 ml of a 1% (w/v) protein solution was homogenized at 16, 000 rpm for 2 min. The mixed sample's volume was measured at 0 and 30 min. To calculate the foaming properties, equations (6) and (7) were employed.

$$\text{FC } (\%) = \frac{\text{V0} - \text{V}}{\text{V}} \times 100 \quad (6)$$

$$\text{FS } (\%) = \frac{\text{V30}}{\text{V0}} \times 100 \quad (7)$$

The protein solution's volume before whipping, after whipping, and after standing is represented by the variables V, V0, and V30, respectively.

2.4.9.4. Water absorption capacity and oil absorption capacity. The

protein samples' water absorption capacity (WAC) and oil absorption capacity (OAC) were determined using a method outlined by Mahalaxmi et al. (2022). WAC and OAC were calculated by dissolving 0.5 g of the sample in 10 ml of deionized water or corn oil. The mixtures were vortexed for 2 min and then centrifuged (2000 g, 10 min) at 25 °C. The extra water or oil was then separated, and the residue was weighed.

WAC or OAC is determined by calculating the difference between the weight of the residue and the weight of the dry sample. This difference is then divided by the weight of the dry sample to obtain the WAC/OAC in grams per gram (g/g).

2.5. Statistical analysis

Data were analyzed using a one-way ANOVA analysis of variance and the statistical software JMP 10. Tukey's test revealed significant differences ($p < 0.05$) between the samples. All experiments were performed in triplicate, and the results are expressed as mean ± SD.

3. Result and discussion

3.1. Effect of modification of zein on secondary structure

The conformational and secondary structural alterations of modified zein were assessed by FTIR analysis (Fig. 1a). Amide groups (I, II, and III) primarily identify structural changes in proteins. The amide I band (1600–1700 cm^{-1}), which results from the stretching of the carbonyl (C=O) group with a partial contribution from the N-H vibration, is associated with an alteration in the protein's secondary structure (Mahalaxmi et al., 2022). Compared to the spectra of samples, various variations in band intensity, band widths, and frequency shifts, especially in the amide I band, were observed. This suggested a change in the zein protein's structure. Random coils were attributed to the band at 1640–1648 cm^{-1}, while β-turns were attributed to the band at 1668–1670 cm^{-1}. The α-helix structure was attributed to the band at 1648–1658 cm^{-1} (Mattice and Marangoni, 2020). The investigation of FTIR absorption intensity in these regions indicated that the chemical modification of zein altered the peaks associated with β-turns, random coils, and α-helixes, leading to protein unfolding, with random coils becoming predominant in the secondary structure. This structural

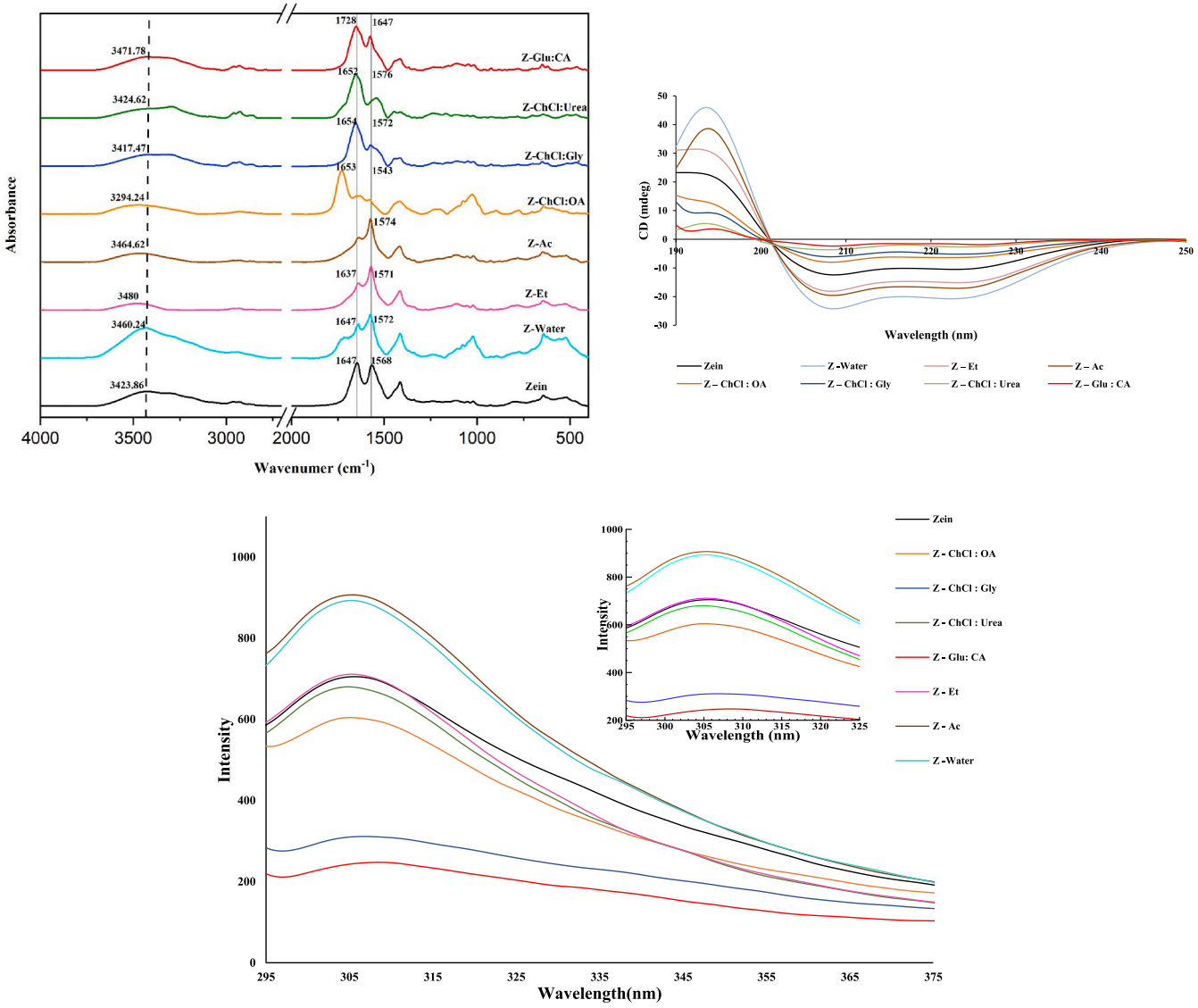

Fig. 1. FT-IR spectra of native and modified zein (a), Circular dichroism spectrum of native and modified zein (b), Fluorescence spectra of native and modified zein (c), UV–visible absorbance spectra of native and modified zein (d).

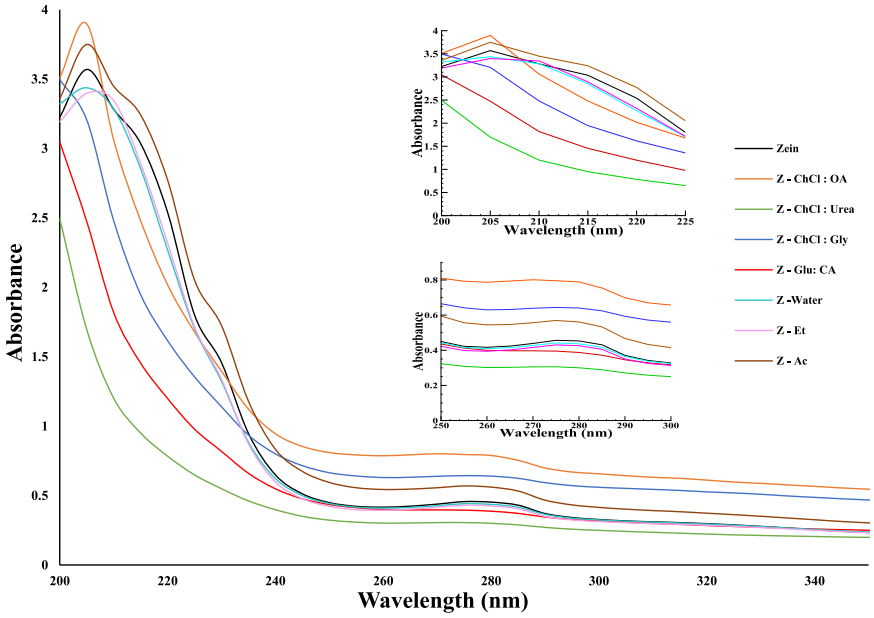

Fig. 1. (*continued*).

alteration may be associated with reactions such as deamidation, which can cause protein molecules to expand and undergo structural changes, shifting from the compressed α-helix to the more flexible or expanded random coils (Zhang et al., 2015). The broad peak at 3650-3200 cm^{-1} indicates the presence of hydroxyl groups (Cao et al., 2021). In comparison to zein (3423.86 cm^{-1}), the vibration of the -OH in Z-ChCl:Gly (3417.47 cm^{-1}) and Z-ChCl:OA (3294.24 cm^{-1}) shifted to lower wavenumbers, as seen in Fig. 1a. This could be attributed to weaker HBs. Disrupting in HBs patterns can alter amide modes' vibrational frequencies, affecting FTIR absorption intensity and indicating unfolded structures (Zhang et al., 2022). A higher negative charge on the molecular chains and fewer HBs may be the origin of these subsequent conformational changes (Zhang et al., 2015). Protein structural expansion is facilitated by the molecule's weaker HBs interactions, which lead to an increase in β-turn content and the exposure of hydrophobic groups in the protein (Zhang et al., 2022). The results of the H_0 value (Table 3) and CD spectra (Table 2) confirmed that the NADES system increased the β-turn content and the H_0 value. Z-ChCl:Urea (3424.62 cm^{-1}), Z-Water (3460.24 cm^{-1}), Z-Ac (3464.62 cm^{-1}), Z-Glu:CA (3471.78 cm^{-1}), and Z-Et (3480 cm^{-1}) all exhibited a red-shift, suggesting the formation of additional HBs (Zheng et al., 2023).

Table 2
Secondary structure of native and modified zein by Circular dichroism spectrum.

Sample	α-helix	β-Sheet	β-Turns	Random Coils
Zein	40.60 ± 0.02^{a}	22.02 ± 0.02^{h}	17.29 ± 0.02^{g}	20.10 ± 0.03^{f}
Z -Water	38.60 ± 0.03^{b}	25.69 ± 0.02^{g}	16.21 ± 0.01^{h}	19.50 ± 0.03^{g}
Z – Et	21.20 ± 0.02^{f}	38.60 ± 0.03^{b}	21.40 ± 0.03^{b}	18.80 ± 0.03^{h}
Z – Ac	15.54 ± 0.02^{g}	42.54 ± 0.03^{a}	21.75 ± 0.03^{a}	20.17 ± 0.01^{e}
Z – ChCl: OA	26.46 ± 0.05^{e}	27.52 ± 0.03^{f}	20.32 ± 0.02^{c}	25.70 ± 0.02^{a}
Z – ChCl: Gly	29.08 ± 0.03^{c}	29.64 ± 0.01^{d}	19.20 ± 0.03^{d}	22.08 ± 0.01^{d}
Z – ChCl: Urea	27.86 ± 0.01^{d}	30.93 ± 0.03^{c}	19.00 ± 0.01^{e}	22.21 ± 0.02^{c}
Z – Glu: CA	27.62 ± 0.01^{d}	29.51 ± 0.02^{e}	18.39 ± 0.02^{f}	24.48 ± 0.01^{b}

* Different letters in each row indicate significantly different mean values ($p < 0.05$).

3.2. CD measurement

CD spectroscopy enables the analysis of protein conformation in its native, unfolded, and partially folded states (Esquembre et al., 2013). As seen in Fig. 1b, the zein spectra displayed two negative peaks at 208 and 221 nm, indicative of an α-helical structure. The change in ellipticity of native zein at 221 nm after chemical modification indicated that solvent-zein interactions significantly influenced its secondary structure. According to Table 2, native zein's secondary structure comprised 17.29% β-turn, 22.02% β-sheet, 40.6% α-helix, and 20.10% random coil. All treatments reduced α-helix content, with Z-Ac showing the lowest (15.54%). This decrease in α-helix content coincided with an increase in β-sheet content, suggesting altered zein binding modes (Dai et al., 2016). Regarding β-sheet and β-turn content, Z-Ac exhibited the highest (42.54% and 21.75%, respectively), while zein and Z-Water showed the lowest (22.02% and 16.21%, respectively). Z-ChCl:OA displayed the highest random coil content (25.70%), whereas Z-Et had the lowest (18.80%).CD spectra revealed that acetic acid, ethanol, and water systems induced partial protein folding with high secondary structure content, while the NADES system resulted in a disordered zein structure. This result is in agreement with other research showing that protein modification using ethanol (Dai et al., 2016), Glu:CA (Cao et al., 2021), and ChCl:Gly and ChCl:Urea (Sanchez-Fernandez et al., 2022) as NADES, can significantly alter protein secondary structures. Fu et al. (2020) reported that NADES modification-induced protein unfolding decreased α-helix and β-turn, while increasing β-sheet and random coil. Additionally, Esquembre et al. (2013) found that ChCl:Gly eutectic solvents lead to partial protein folding with high secondary structure content, whereas urea-based DES tend to destabilize protein structures more extensively under thermal treatment.

3.3. Tertiary structure

3.3.1. Fluorescence absorption spectra

Fluorescence parameters of aromatic chromophores, such as tryptophan, tyrosine, and phenylalanine, can be used to probe protein structure (Antosiewicz and Shugar, 2016). Tyrosine residues are abundant in zein, which typically has an emission maximum wavelength (λ_{max}) of about 304 nm (Dai et al., 2016). Tyrosine residue fluorescence spectra at 295–375 nm in both natural and modified zein reveal details

Table 3
Free sulfhydryl, Disulfide bond, Free amine, and Surface hydrophobicity of native and modified zein.

Treatment	Free sulfhydryl (μmol/g)	Disulfide bond (μmol/g)	Free amine content (mM)	Surface hydrophobicity
Zein	3.40 ± 0.08^{ab}	11.97 ± 0.06^{b}	0.05 ± 0.01^{ef}	2464.33 ± 9.07^{h}
Z -Water	3.53 ± 0.07^{ab}	13.11 ± 0.13^{ab}	0.07 ± 0.00^{ef}	2756 ± 12.12^{f}
Z - Et	3.08 ± 0.17^{bc}	7.53 ± 0.19^{d}	0.17 ± 0.00^{e}	3552.73 ± 9.48^{e}
Z - Ac	3.19 ± 0.14^{bc}	14.09 ± 0.20^{a}	0.05 ± 0.01^{f}	7304.8 ± 6.34^{b}
Z - ChCl:OA	3.84 ± 0.39^{a}	8.25 ± 0.26^{c}	2.96 ± 0.07^{a}	11475.67 ± 7.57^{a}
Z - ChCl:Gly	3.21 ± 0.08^{bc}	4.83 ± 0.39^{d}	1.26 ± 0.03^{b}	4187.5 ± 11.20^{d}
Z - ChCl:Urea	2.86 ± 0.04^{c}	3.80 ± 0.16^{de}	0.69 ± 0.02^{d}	2494.63 ± 4.10^{g}
Z - Glu:CA	3.06 ± 0.03^{bc}	2.80 ± 0.08^{e}	0.9 ± 0.08^{c}	5072.86 ± 7.63^{c}

* Different letters in each row indicate significantly different mean values ($p < 0.05$).

on the protein's folding state and alterations to its tertiary structure (Cui et al., 2022). Z-Ac exhibited the highest emission peak at 305 nm, while Z-Glu:CA displayed the lowest (Fig. 1c). In addition, the fluorescence intensity of zein modified by the NADES system was lower than in the acetic acid, ethanol, and water systems, confirming the existence of alterations in the zein amino acid sequence (Glusac et al., 2018). The NADES disrupts protein HBs, facilitating the formation of HBs between the protein and HBD or HBA (Zheng et al., 2023; Sanchez-Fernandez et al., 2022). This process partially unfolds the protein conformation, exposing tyrosine residues on its surface (Fu et al., 2020). Furthermore, the exposed aromatic amino acid residues may interact with choline-based NADES, leading to the quenching of intrinsic fluorescence and a subsequent decrease in fluorescence intensity (Sanchez-Fernandez et al., 2022). Additionally, it is possible that the quenching of the fluorescence emission of aromatic chromophores is due to Förster resonance energy transfer (FRET). Since fluorophores have overlapping excitation and emission spectra, FRET can occur between these amino acids (Sadat et al., 2022). Ghisaidoobe and Chung (2014) found that the fluorescence intensity of tryptophan residues in proteins decreases when the proteins unfold and expose their residues to a hydrophilic environment. Fu et al. (2020) found that glycated bovine serum albumin fluorescence intensity in the NADES system was lower than in the water system, indicating that the NADES system produced more quenching agents.

3.3.2. *UV–visible absorption spectra*

UV–Vis light absorption, emission, and scattering, along with the optical properties of the tyrosine chromophore, are used to investigate protein conformational changes (Antosiewicz and Shugar, 2016). The UV absorption peak at 205 nm and 280 nm in zein protein was observed. The 205 nm peak likely arises from n-π^* electronic transitions within the protein's carbonyl groups, while the 280 nm peak results from the electronic transition of π-π* and n-π* of tyrosine in the peptide bond (Meng et al., 2022). Z-ChCl:OA had the maximum UV–visible absorbance at 205 and 280 nm, while Z-ChCl:Urea had the lowest absorbance (Fig. 1d). At 205 nm, the peak of Z-ChCl:OA was higher than the peaks of Z-Water, Z-Ac, and Z-Et. In contrast, at 280 nm, the peaks of Z-ChCl:OA and Z-ChCl:Gly were higher than those of these solvents. UV–visible absorbance spectra changes are associated with protein conformational changes triggered by the exposure of buried aromatic residues when the amino acid environment alters (Sanchez-Fernandez et al., 2022). Cao et al. (2021) reported that the NADES system disrupts HBs in protein molecules, leading to protein unfolding and expansion of conformation, resulting in UV–visible absorbance spectra changes.

3.4. *Interactions between proteins*

Based on the solubility of samples in PBS, urea, thiourea, and DTT solutions (Fig. 3a), we evaluated the effects of various protein interactions. These solutions can change both covalent and noncovalent bonds (Dent et al., 2023). PBS, the primary extraction buffer used here, is known to extract proteins while preserving their native state (Zheng et al., 2015). Adding the other solutions increased protein solubility, with zein reaching approximately 6.23% solubility in PBS. The NADES system showed reduced solubility when dissolved in urea and thiourea solutions, indicating that HBs and hydrophobic interactions are the main contributors to this decrease. Conversely, solubility increased in water, ethanol, and acetic acid systems, with Z-Ac demonstrating the highest solubility in urea (84.87%) and thiourea (25.59%). In contrast, Z-Glu:CA and Z-ChCl:OA exhibited the lowest solubility in these solvents (35.36% and 8.85%, respectively). These results suggest that chemical treatment altered the arrangement of hydrophobic interactions and HBs in zein. The mechanism of NADES-protein interactions involves various interactions: hydrophobic interactions facilitate protein solubilization, ionic NADES ingredients interact electrostatically with charged amino acid residues, and HBs takes place between the HBD component and protein amino acid residues (Karabulut et al., 2024). Furthermore, chemical modifications can alter protein charge, disrupting the HBs that stabilize protein structure, leading to complex protein dissociation and exposing more buried groups (Karimi et al., 2024; Zheng et al., 2023). Thiourea may reduce solubility, indicating that modifications to hydrophobic interactions can destabilize protein structures, a process influenced by the hydrophobic effect (Dent et al., 2023). DTT interfered with disulfide bonds, resulting in the creation of covalent bonds. Modifying with NADES decreased protein solubility in DTT, while Z-Ac and Z-Water increased solubility. Remarkably, Z-Ac exhibited the highest solubility at 20.62%, while Z-Glu had the lowest at 2.73%, suggesting that Z-Ac may promote the formation of additional disulfide bonds. Urea and DTT exhibit a synergistic interaction, as their combined effect on protein solubility, by breaking both covalent and non-covalent bonds, is much larger than greater than the effect of either solvent individually (Chen et al., 2021). Nonetheless, adding urea can modify protein structure by altering non-covalent interactions that may expose previously hidden disulfide bonds to DTT (Zheng et al., 2015). Among these solvents, Z-Ac and Z-Glu showed the highest (99.19%) and lowest (64.59%) solubility, respectively. Nonetheless, it was observed that hydrogen bonding interactions have a more pronounced impact on the chemical modification of zein than disulfide bond alterations.

3.5. *Free amine group content*

Table 3 shows the impact of chemical modification on the free amino groups of zein. Because native zein's compact structure and unbroken peptide bonds limit reagent access, it has a low free amine concentration (0.05 mM). In alcohol-based solvents, this hydrophobic protein assembles into larger, compressed, and spiral conformations (He et al., 2021). Additionally, Z-Et, Z-Water, and Z-Ac revealed low levels of free amines. However, the NADES system increased the amount of free amine compared to these solvents, with Z-ChCl:OA having the highest free amine content (2.96 mM). HBs can be formed between the amino or carboxyl groups of proteins and HBA and HBD (Cao et al., 2023), thus disrupting existing HBs between amine groups and other molecules, revealing buried groups like hydrophobic and amine groups, leading to protein unfolding (Zheng et al., 2023; Wu et al., 2021). Additionally, H^+ from HBs in NADES molecules, or from deprotonation of the COOH group of HBD like citric acid and oxalic acid, can increase the accessibility of protein amide groups for nucleophilic assault, assisting their

removal. Furthermore, NADES increases the space available for a hydrophilic environment, thereby promoting protein unfolding and expansion of its conformation. This improves the interaction between H^+ and amide groups and leads to a reaction likely deamidation, which ultimately increases free amine content (He et al., 2021; Cao et al., 2021). Zheng et al. (2022), found that wheat gluten deamidation by NADES enhances functional properties, particularly emulsification and foaming properties. Additionally, HBs between NADES and protein unfold the structure and make it more flexible. This increases H^+ ionization, which enhances amide group availability and could lead to an increase in free amine content.

3.6. Free sulfhydryl groups and disulfide bonds

Sulfhydryl and disulfide bonds are key functional groups in food-based proteins, with the ability to convert between each other (Liu et al., 2023). Table 3 shows the change in protein free sulfhydryl groups and disulfide bonds of native and modified zein. Z-Ac revealed a higher disulfide content (14.09 ± 0.20 μmol/g) and solubility in DTT (Fig. 3a). This is related to the ability of free sulfhydryl groups to oxidize and form disulfide bonds with other sulfhydryl groups (Liu et al., 2023). In contrast, the NADES system specifically disrupts disulfide bonds and weakens internal HBs interactions, as confirmed by the increased solubility of the protein in the DDT and urea extractant. On the other hand, disulfide bonds maintain the tertiary structure of proteins (Liu et al., 2023). Therefore, the changes in zein's tertiary structure, confirmed by fluorescence and UV–visible absorption spectroscopy, suggest that chemical modifications affect disulfide bonds. Zein modified by NADES showed lower disulfide bonds and better functional properties than other treatments. Wu et al. (2021) found that reducing disulfide bond formation weakened the protein molecule's internal structure, improved the interaction between the protein membrane and the oil droplets, and significantly affected the protein-stabilized emulsions. Zheng et al. (2023) found that super-deamidated wheat gluten prepared using NADES exhibited conformational alterations. These modifications reduced disulfide bonds and increased low-molecular-weight units, improving oil droplet stability and microstructure in a model emulsion by expanding protein structures and exposing hydrophobic groups through weakened HBs. Additionally, this process exposed more cysteine residues, improving the protein's hydrophilicity and water solubility.

3.7. Surface hydrophobicity (H_0)

H_0 represents changes in protein structure and functional characteristics by measuring the extent of protein unfolding and hydrophobic group exposure to the solvent (Cao et al., 2023; Cui et al., 2022). Table 3 shows the H_o values of native and modified zein treated with different chemical solutions. All treatments exhibited significantly higher H_o values than native zein, with Z-ChCl:OA exhibiting the highest value (11475.66). A higher H_0 value indicates enhanced solubility, reduced aggregation tendency, and potential exposure of hydrophobic regions for ANS fluorescence binding (Zhao et al., 2012). NADES disrupts the internal HBs of the protein, revealing buried hydrophobic groups. Additionally, NADES increases HBs between the protein and the HBD or HBA components, leading to protein unfolding and an altered H_0 value (Zheng et al., 2023; Wu et al. (2021). A positive correlation ($r = 0.87$) was found between protein H_0 and emulsifying activity, suggesting that proteins with higher H_0 are more effective emulsifiers due to their enhanced surface activity (Aewsiri et al., 2009). Moreover, Cao et al. (2023) reported that NADES treatment significantly increased the H_0 of sesame protein. This is likely attributed to the varying pH values of different NADES, which influence the exposure of internal polar and hydrophobic groups. Furthermore, the varied H_0 values seen across treatments are most likely caused by electrostatic repulsion in solutions, which encourages the hydrophobic groups on the protein's surface to get accessible (Cao et al., 2023). The results of the interactions between proteins (Fig. 3a) reveal that the NADES system has decreased hydrophobic interactions compared to other solvents, leading to increased exposure of hydrophobic groups, which destabilizes protein structures.

3.8. SDS-PAGE

Electrophoretic analysis is used to study protein subunit molecular weight distribution (Cui et al., 2022). Native zein, Z-Water, Z-Et, and Z-Ac exhibited similar patterns with broad bands at 14 kDa, 16–18 kDa, 19–22 kDa, and 41 kDa, as shown in Fig. 2. Additionally, thin bands at 42–48 kDa represented dimers. Z-ChCl:OA and Z-Glu:CA showed no increase in molecular weight. NADES systems demonstrate a reduction in HBs and hydrophobic interactions (Fig. 3a), which results in decreased molecular weight of proteins. This reduction is due to the lack of intramolecular HBs, enabling the protein to depolymerize (Liu et al., 2018). Z-ChCl:Urea and Z-ChCl:Gly formed bonds at higher range, resulting in high molecular weight. Chemical modification of zein can affect the molecular weight of proteins by altering their conformation (Nonthanum et al., 2013). Cao et al. (2021) found that modifying wheat gluten with NADES results in minimal depolymerization of α-, β-, and γ-gliadins, enhancing deamidation. NADES systems can decrease the molecular weight of proteins by breaking peptide bonds or other covalent bonds in the protein backbone (Cao et al., 2021). In contrast, Lores et al. (2017) reported that NADES did not disrupt wheat gluten structure.

3.9. Functional properties

3.9.1. Protein solubility

Protein solubility is crucial for its various functions including, forming gels, foaming, and emulsifying (Hu and Li, 2022). The solubility of native and modified zein in alkaline, neutral, and acidic solutions is presented in Fig. 3b. At the isoelectric point, electrostatic interactions make hydrophobic groups stronger. This makes the protein structure more compact and reduces its functional properties, especially its solubility (Cao et al., 2023). Zein has low solubility in water at pH 7.0 (10.62%) because it is near its isoelectric point (pH 6.2). Moreover, protein solubility improves as pH above or below the isoelectric point, disrupting protein aggregates (Zhao et al., 2012). Results revealed that zein modified with NADES exhibited higher solubility at pH 7.0 and pH 10.0 levels compared to zein modified with water, ethanol, or acetic acid. Z-Ac and Z-Et exhibited low solubility and high β-sheet content

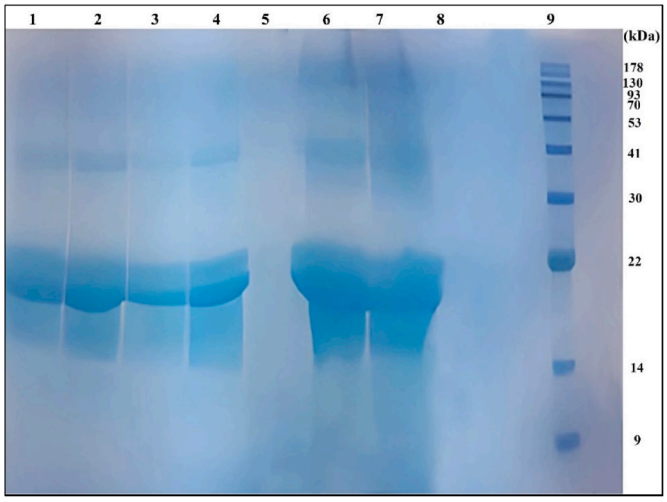

Fig. 2. SDS-PAGE of native and modified zein. Lane 1) native zein; 2) Z-Water; 3) Z-Et; 4) Z-Ac; 5) Z-ChCl:OA; 6) Z-ChCl:Urea; 7) Z-ChCl:Gly; 8) Z-Glu:CA and 9) Marker.

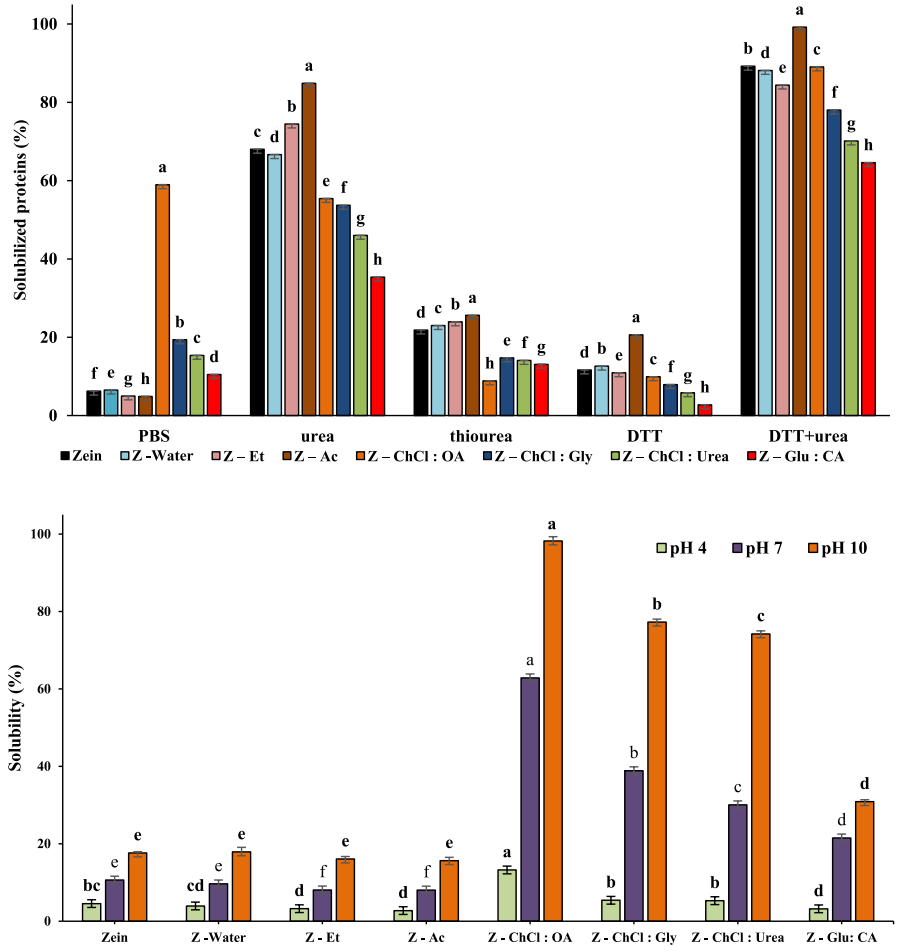

Fig. 3. Protein solubility of native and modified zein in solvent systems of PBS, urea, thiourea, DTT, and DTT + urea (a), Solubility of native and modified zein at pH 4.0, pH 7.0, and pH 10.0 (b). Data are means ± SD of three replicates. Values with different letters are significantly different ($p < 0.05$).

(Table 2), indicating that aggregation may have occurred, which could lead to decreased solubility. Various NADES have different impacts on solubility because of their diverse physical and chemical characteristics (Cao et al., 2023). Z-ChCl:OA showed the highest solubility (13.22%, 62.85%, and 98.22% at pH 4.0, 7.0, and 10.0, respectively). It could be associated with the ChCl:OA system, which may have interacted with the proline imino group in zein, whereas other NADES may establish HBs with the amino or carboxyl groups of different amino acids (Cao et al., 2023). Additionally, as the protein unfolds in NADES, the strong electrostatic repulsion between the unfolded proteins helps prevent extreme aggregation, leading to enhanced solubility (Cao et al., 2023). Partially unfolded protein molecules that are confirmed by the result of fluorescence and FTIR spectra may have caused the compact structure of the protein to separate, revealing more polar residues on the surface. This alteration can enhance protein solubility without excessively exposing non-polar amino acids, which could lead to aggregation (Karimi et al., 2024).

3.9.2. Emulsifying properties

Emulsifying properties are affected by the molecular weight of the substance, charge, solubility, and hydrophobicity (Cao et al., 2023). Native zein had a low EAI (5.57 m^2/g), indicating poor emulsifying properties due to lack of surface activity. No significant variation was found in the EAI of native zein, Z-Water, and Z-Et. The choline chloride-based NADES system exhibited a significantly higher ESI value than those obtained using water, ethanol, and acetic acid systems ($p < 0.05$). Z-ChCl:OA and Z-ChCl:Gly showed the highest EAI (50.86 m^2/g) and ESI (99.22%), respectively (Fig. 4a and b). High solubility accelerates the dispersion and adsorption at the interface, which leads to improved emulsifying properties ($r = 0.84$) (Hu and Li, 2022). Z-ChCl:OA exhibited the highest solubility (Fig. 3) and EAI. This enhanced functionality might be due to the strong electrostatic repulsion between unfolded proteins, which prevents excessive aggregation and improves emulsification (Cao et al., 2023). When protein molecules unfold, the majority of their hidden hydrophobic functional groups are revealed, reducing the interfacing energy between the water and oil phases and enhancing emulsification (Cao et al., 2023). The strongest ESI results from sufficient hydrophobicity on the surface and structural flexibility, which maintain the water-oil interaction equilibrium (Zheng et al., 2023). Also, the increased hydrophilicity of the protein exposes more hydrophobic amino acids, enhancing its emulsification properties (Cabra et al., 2007).

3.9.3. Foaming properties

Hydrophobicity, Proteins' structural flexibility, and solubility all affect their foaming features (Cao et al., 2023). FC is primarily affected by a protein's strong foaming ability, while FS is influenced by the amount of denatured protein (Kumar et al., 2014). Zein exhibited the lowest FC (10.62%) among all samples ($p < 0.05$) (Fig. 4c). Although Z-Et, Z-Water, and Z-Ac improved FC compared to native zein, the

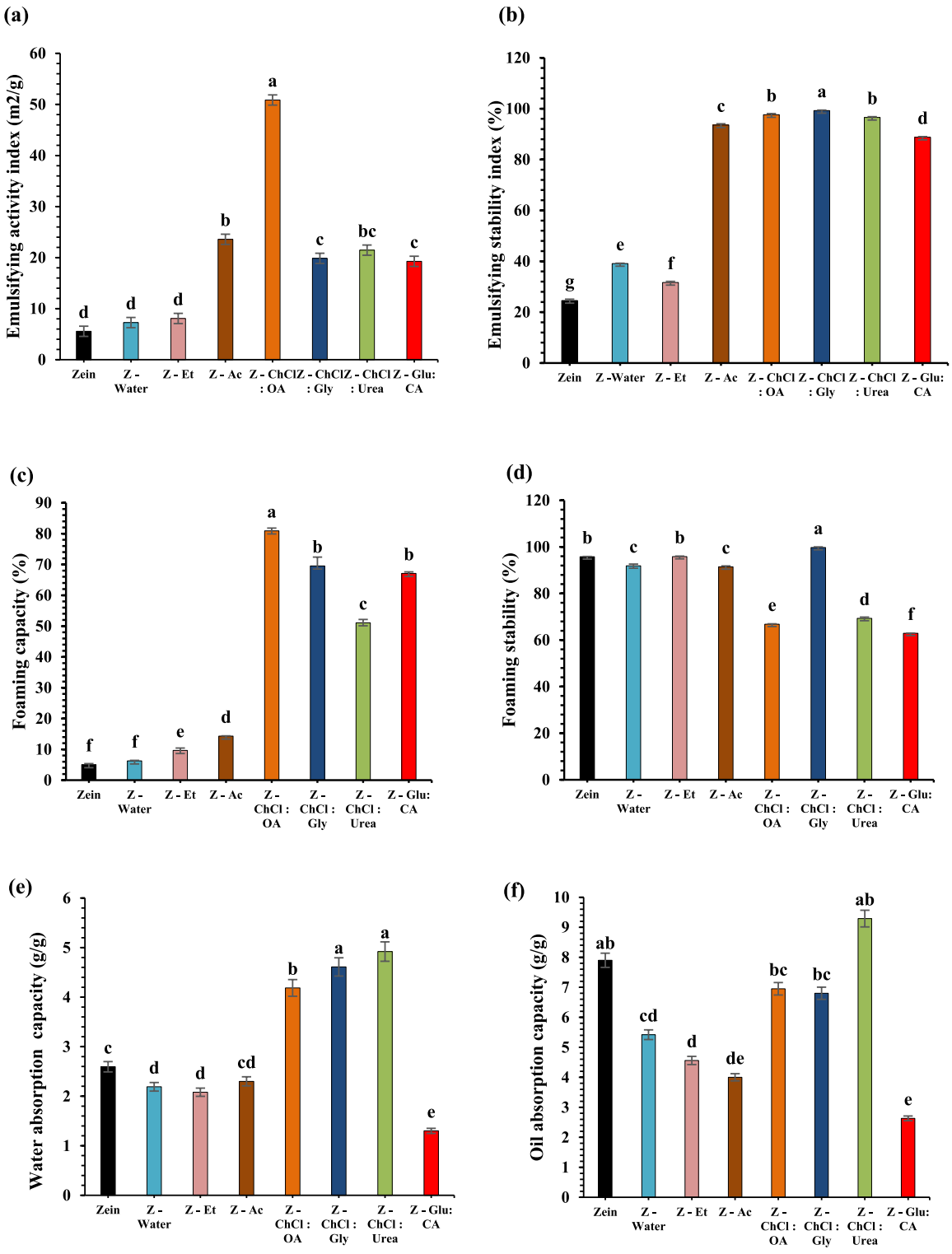

Fig. 4. Emulsifying activity (a) and stability (b), Foaming capacity (c) and stability (d), Water absorption capacity (e), and Oil absorption capacity (f) of native and modified zein. Data are means ± SD of three replicates. Values with different letters are significantly different ($p < 0.05$).

NADES system led to an even greater increase in FC. Solubility and changes in protein conformation affect foam properties. A positive relationship (r = 0.8), was observed between protein FC and solubility at pH 7.0. Z-ChCl:OA exhibited the highest FC (80.90%) due to its high solubility. The increased net charge on the protein surface, resulting from unfolding, impacts hydrophobic interactions between protein molecules. This enables the protein to diffuse to the air-water interface, enhancing foaming properties rapidly (Jiang et al., 2024). In contrast, Z-ChCl:Gly displayed the highest FS (99.75%) (Fig. 4d), which may be attributed to the protein forming a stronger layer around the bubble than other samples. This is likely due to a better balance of hydrophobic and hydrophilic groups (Zheng et al., 2023). The NADES system offers

functional advantages with a preferred structural modification without significantly affecting stability. Compared to other solvents, NADES offers better FC and FS, suggesting that these solvents modify the protein structure to enhance air trapping and emulsion formation while maintaining stability (Karabulut et al., 2024). Yue et al. (2021) suggest that the enhanced FC and FS of proteins extracted by NADES may be partly attributed to their high solubility, which is generally positively correlated with FC.

3.9.4. Water absorption capacity and oil absorption capacity

The WAC and OAC of proteins are associated with texture, making them crucial attributes in the food processing industry (Hu and Li, 2022). The findings demonstrated that zein modification affected both WAC and OAC (Fig. 4e and f). Native zein exhibits varying WAC (1.3–4.92 g/g) and OAC (2.63–9.29 g/g), whereas modified zein has a WAC of 2.59 g/g and an OAC of 7.9 g/g. The amount of WAC and OAC in NADES systems, except for Z-Glu:CA, was higher than in Z-Et, Z-Water, and Z-Ac. The Z-ChCl:Urea revealed the highest WAC and OAC values (4.92 g/g and 9.29 g/g, respectively). Cao et al. (2023) reported proteins modified by NADES improved WAC and OAC. When a protein dissolves, it forms a complex network structure capable of entrapping water molecules, thereby enhancing WAC (Cao et al., 2023). Additionally, protein unfolding exposes additional hydrophilic regions, further increasing WAC. Notably, the disruption of β-turn and random coil secondary structures significantly contributes to this effect (Mahalaxmi et al., 2022). Furthermore, a protein's capacity to interact with non-polar groups, quantified by its OAC, is significantly influenced by its non-polar side chain exposure (Cao et al., 2023). Modifying protein structure using organic solvents can enhance OAC by exposing buried non-polar amino acids and hydrophobic regions (Mahalaxmi et al., 2022). Conversely, this process can disrupt the balance between hydrophobic and hydrophilic residues due to the inevitable unfolding of the protein conformation, resulting in a decrease in both WAC and OAC (Ogunbusola et al., 2022).

4. Conclusions

Chemical modification with NADES significantly altered the secondary and tertiary structure of zein. This was evidenced by the altered UV–visible absorbance spectra, decreased fluorescence intensity, and changes in secondary structure seen in CD spectra, notably an increase in random coil content and a decrease in α-helix content. The effect of NADES on disulfide bonds was dependent on the specific HBA/HBD combination used. Z-Ac treatment increased disulfide content, while NADES systems showed no significant difference compared to native zein. SDS-PAGE analysis revealed that NADES modification with ChCl:Urea and ChCl:Gly formed high molecular weight aggregates, while other NADES systems had no significant effect on molecular weight. Z-ChCl:OA exhibited the highest solubility across all pH values. Z-ChCl:OA and Z-ChCl:Gly showed the highest EAI and ESI, respectively. In general, modified zein by ChCl:OA showed better properties than zein modified by ethanol, acetic acid, and other NADES.

CRediT authorship contribution statement

Adieh Anvar: Investigation, Methodology, Data curation, Writing – original draft. **Mohammad Hossein Azizi:** Supervision, Writing – review & editing. **Hassan Ahmadi Gavlighi:** Supervision, Writing – review & editing.

Declaration of competing interest

The authors declare that they have no known competing financial interests or personal relationships that could have appeared to influence the work reported in this paper.

Acknowledgments

This work is based upon research funded by Iran National Science Foundation (INSF) under project No.4005843.

Data availability

Data will be made available on request.

References

2000 AACC, 2000. In: *Approved methods of the American Association of Cereal Chemists*, 2000, 10th ed. The American Association of Cereal Chemists, St. Paul, MN.

Aewsiri, T., Benjakul, S., Visessanguan, W., Eun, J.B., Wierenga, P.A., Gruppen, H., 2009. Antioxidative activity and emulsifying properties of cuttlefish skin gelatin modified by oxidised phenolic compounds. Food Chem. 117 (1), 160–168. https://doi.org/10.1016/j.foodchem.2009.03.092.

Antosiewicz, J.M., Shugar, D., 2016. UV–Vis spectroscopy of tyrosine side-groups in studies of protein structure. Part 2: selected applications. Biophys Rev 8, 163–177. https://doi.org/10.1007/s12551-016-0198-6.

Anvar, A., Azizi, M.H., Gavlighi, H.A., 2024. Enhancing zein functionality through sequential limited Alcalase hydrolysis and transglutaminase treatment: structural changes and functional properties. Food Chem. X 24, 101957. https://doi.org/10.1016/j.fochx.2024.101957.

Bean, S.R., Akin, P.A., Aramouni, F.M., 2021. Zein functionality in viscoelastic dough for baked food products. J. Cereal. Sci. 100, 103270. https://doi.org/10.1016/j.jcs.2021.103270.

Bradford, M.M., 1976. A rapid and sensitive method for the quantitation of microgram quantities of protein utilizing the principle of protein-dye binding. Anal. Biochem. 72 (1–2), 248–254. https://doi.org/10.1016/0003-2697(76)90527-3.

Cabra, V., Arreguin, R., Vazquez-Duhalt, R., Farres, A., 2007. Effect of alkaline deamidation on the structure, surface hydrophobicity, and emulsifying properties of the Z19 α-zein. J. Agric. Food Chem. 55 (2), 439–445. https://doi.org/10.1021/jf061002r.

Cao, S.L., Zheng, W.Y., Chen, Z.P., Zhang, F.L., Jiang, W.H., Qiu, Y.Q., Gu, M., Chen, Z., Zheng, T., Zhang, H., Wang, S., Liao, L., 2021. Highly efficient deamidation of wheat gluten by glucose-citric acid-based natural deep eutectic solvent: a potential effective reaction media. J. Agric. Food Chem. 69 (11), 3452–3465. https://doi.org/10.1021/acs.jafc.0c07275.

Cao, P.H., Zhang, C.X., Ma, Y.X., Yu, Y.M., Liu, H.M., Wang, X.D., Zheng, Y.Z., 2023. Extraction of protein from sesame meal: impact of deep eutectic solvents on protein structure and functionality. LWT 115366. https://doi.org/10.1016/j.lwt.2023.115366.

Chen, D., Zhu, X., Ilavsky, J., Whitmer, T., Hatzakis, E., Jones, O.G., Campanella, O.H., 2021. Polyphenols weaken pea protein gel by formation of large aggregates with diminished noncovalent interactions. Biomacromolecules 22 (2), 1001–1014. https://doi.org/10.1021/acs.biomac.0c01753.

Cui, Q., Liu, J., Wang, G., Zhang, A., Wang, X., Zhao, X.H., 2022. Effect of freeze-thaw treatment on the structure and texture of soy protein-dextran conjugate gels crosslinked by transglutaminase. LWT 153, 112443. https://doi.org/10.1016/j.lwt.2021.112443.

Dai, L., Sun, C., Wang, D., Gao, Y., 2016. The interaction between zein and lecithin in ethanol-Water solution and characterization of zein-Lecithin composite colloidal nanoparticles. PLoS One 11 (11), e0167172. https://doi.org/10.1371/journal.pone.0167172.

Dent, T., Campanella, O., Maleky, F., 2023. Enzymatic hydrolysis of soy and chickpea protein with Alcalase and Flavourzyme and formation of hydrogen bond mediated insoluble aggregates. Curr. Res. Food Sci. 6, 100487. https://doi.org/10.1016/j.crfs.2023.100487.

Dong, S.R., Xu, H.H., Ma, J.Y., Gao, Z.W., 2020. Enhanced molecular flexibility of α-zein in different polar solvents. J. Cereal. Sci. 96, 103097. https://doi.org/10.1016/j.jcs.2020.103097.

Esquembre, R., Sanz, J.M., Wall, J.G., del Monte, F., Mateo, C.R., Ferrer, M.L., 2013. Thermal unfolding and refolding of lysozyme in deep eutectic solvents and their aqueous dilutions. Phys. Chem. Chem. Phys. 15 (27), 11248–11256. https://doi.org/10.1039/c3cp44299c.

Fu, J.J., Sun, C., Xu, X.B., Zhou, D.Y., Song, L., Zhu, B.W., 2020. Improving the functional properties of bovine serum albumin-glucose conjugates in natural deep eutectic solvents. Food Chem. 328, 127122. https://doi.org/10.1016/j.foodchem.2020.127122.

Ghisaidoobe, A.B., Chung, S.J., 2014. Intrinsic tryptophan fluorescence in the detection and analysis of proteins: a focus on Förster resonance energy transfer techniques. Int. J. Mol. Sci. 15 (12), 22518–22538. https://doi.org/10.3390/ijms151222518.

Glusac, J., Fishman, A., 2021. Enzymatic and chemical modification of zein for food application. Trends Food Sci 112, 507–517. https://doi.org/10.1016/j.tifs.2021.04.024.

Glusac, J., Davidesko-Vardi, I., Isaschar-Ovdat, S., Kukavica, B., Fishman, A., 2018. Gel-like emulsions stabilized by tyrosinase-crosslinked potato and zein proteins. Food Hydrocoll 82, 53–63. https://doi.org/10.1016/j.foodhyd.2018.03.046.

He, W., Tian, L., Fang, F., Chen, D., Federici, E., Pan, S., Jones, O.G., 2021. Limited hydrolysis and conjugation of zein with chitosan oligosaccharide by enzymatic reaction to improve functional properties. Food Chem. 348, 129035. https://doi.org/10.1016/j.foodchem.2021.129035.

Hu, A., Li, L., 2022. Effects of ultrasound pretreatment on functional property, antioxidant activity, and digestibility of soy protein isolate nanofibrils. Ultrason. Sonochem. 90, 106193. https://doi.org/10.1016/j.ultsonch.2022.106193.

Jiang, X., Gao, F., Ma, Y., Huo, N., Guo, Y., Yu, Y., 2024. Protein from tiger nut meal extracted by deep eutectic solvent and alkali-soluble acid precipitation: a comparative study on structure, function, and nutrition. Food Chem. 452 (5333), 139608. https://doi.org/10.1016/j.foodchem.2024.139608.

Karabulut, G., Köroğlu, D.G., Feng, H., Karabulut, Z., 2024. Sustainable fungi-based protein extraction from agro-waste mushroom stem using deep eutectic solvents. Food Chem. X, 101931. https://doi.org/10.1016/j.fochx.2024.101931.

Karimi, A., Bhowmik, P., Yang, T.C., Samaranayaka, A., Chen, L., 2024. Extraction of canola protein via natural deep eutectic solvents compared to alkaline treatments: isolate characteristics and protein structural and functional properties. Food Hydrocoll 152, 109922. https://doi.org/10.1016/j.foodhyd.2024.109922.

Kumar, K.S., Ganesan, K., Selvaraj, K., Rao, P.S., 2014. Studies on the functional properties of protein concentrate of *Kappaphycus alvarezii* (Doty) Doty–An edible seaweed. Food Chem. 153, 353–360. https://doi.org/10.1016/j.foodchem.2013.12.058.

Liu, Y., Chi, Y., Chi, Y., 2023. Water filling of rapidly salted separated egg yolks: characterization of water migration, aggregation behavior, and protein structure. Food Chem Adv 2, 100274. https://doi.org/10.1016/j.focha.2023.100274.

Liu, Y., Zhang, L., Li, Y., Yang, Y., Yang, F., Wang, S., 2018. The functional properties and structural characteristics of deamidated and succinylated wheat gluten. Int. J. Biol. Macromol. 109, 417–423. https://doi.org/10.1016/j.ijbiomac.2017.11.175.

Lores, H., Romero, V., Costas, I., Bendicho, C., Lavilla, I., 2017. Natural deep eutectic solvents in combination with ultrasonic energy as a green approach for solubilization of proteins: application to gluten determination by immunoassay. Talanta 162, 453–459. https://doi.org/10.1016/j.talanta.2016.10.078.

Lowry, O., Rosebrough, N., Farr, A.L., Randall, R., 1951. Protein measurement with the Folin phenol reagent. J. Biol. Chem. 193 (1), 265–275. https://doi.org/10.1016/S0021-9258(19)52451-6.

Mahalaxmi, S., Himashree, P., Malini, B., Sunil, C.K., 2022. Effect of microwave treatment on the structural and functional properties of proteins in lentil flour. Food Chem Adv 1, 100147. https://doi.org/10.1016/j.focha.2022.100147.

Mattice, K.D., Marangoni, A.G., 2020. Functionalizing zein through antisolvent precipitation from ethanol or acetic acid. Food Chem. 313, 126127. https://doi.org/10.1016/j.foodchem.2019.126127.

Meng, Y., Xue, Q., Chen, J., Li, Y., Shao, Z., 2022. Structure, stability, rheology, and texture properties of ε-polylysine-whey protein complexes. J. Dairy Sci. 105 (5), 3746–3757. https://doi.org/10.3168/jds.2021-21219.

Negi, T., Kumar, A., Kumar, S., Rawat, N., Saini, D., 2024. Heliyon Deep eutectic solvents : preparation, properties, and food applications. Heliyon 10 (7), e28784. https://doi.org/10.1016/j.heliyon.2024.e28784.

Nonthanum, P., Lee, Y., Padua, G.W., 2013. Effect of pH and ethanol content of solvent on rheology of zein solutions. J. Cereal. Sci. 58 (1), 76–81. https://doi.org/10.1016/j.jcs.2013.04.001.

Ogunbusola, E.M., Alabi, O.O., Araoye, K.T., Sanni, T.A., Jaiyeoba, C.N., Adebayo-Alabi, I.B., Akila, O.A., 2022. Impact of extraction methods on the quality, physicochemical, and functional properties of white melon (*Cucumeropsis mannii*) seed protein concentrates. Food Chem Adv 1, 100131. https://doi.org/10.1016/j.focha.2022.100131.

Qu, W., 2019. DES Modified Protein-Based Materials and Their Use in Pharmaceutical Applications (Doctoral Dissertation, University of Leicester).

Sadat, A., Corradini, M.G., Joye, I.J., 2022. Vibrational and fluorescence spectroscopy to study gluten and zein interactions in complex dough systems. Curr. Res. Food Sci. 5, 479–490. https://doi.org/10.1016/j.crfs.2022.02.009.

Sanchez-Fernandez, A., Basic, M., Xiang, J., Prevost, S., Jackson, A.J., Dicko, C., 2022. Hydration in deep eutectic solvents induces non-monotonic changes in the conformation and stability of proteins. J. Am. Chem. Soc. 144 (51), 23657–23667. https://doi.org/10.1021/jacs.2c11190.

Shishov, A., Makoś-Chełstowska, P., Bulatov, A., Andruch, V., 2022. Deep eutectic solvents or eutectic mixtures? Characterization of tetrabutylammonium bromide and nonanoic acid mixtures. J. Phys. Chem. B 126 (21), 3889–3896. https://doi.org/10.1021/acs.jpcb.2c00858.

Sun, X., Ohanenye, I.C., Ahmed, T., Udenigwe, C.C., 2020. Microwave treatment increased protein digestibility of pigeon pea (*Cajanus cajan*) flour: elucidation of underlying mechanisms. Food Chem. 329, 127196. https://doi.org/10.1016/j.foodchem.2020.127196.

Wu, M., Li, Z., Wei, R., Luan, Y., Hu, J., Wang, Q., Liu, R., Ge, Q., Yu, H., 2021. Role of disulfide bonds and sulfhydryl blocked by n-ethylmaleimide on the properties of different protein-stabilized emulsions. Foods 10 (12), 3079. https://doi.org/10.3390/foods10123079.

Yap, P.G., Gan, C.Y., 2024. Exploration of potential application of low phytotoxic alkaline deep eutectic solvent (DES) in protein extraction and bioactive applications. J. Mol. Liq. 409, 125521. https://doi.org/10.1016/j.molliq.2024.125521.

Yue, J., Zhu, Z., Yi, J., Lan, Y., Chen, B., Rao, J., 2021. Structure and functionality of oat protein extracted by choline chloride–dihydric alcohol deep eutectic solvent and its water binary mixtures. Food Hydrocoll 112, 106330. https://doi.org/10.1016/j.foodhyd.2020.106330.

Yu, J., Xu, S., Goksen, G., Yi, C., Shao, P., 2023a. Chitosan films plasticized with choline-based deep eutectic solvents: UV shielding, antioxidant, and antibacterial properties. Food Hydrocoll 135. https://doi.org/10.1016/j.foodhyd.2022.108196.

Yu, J., Chen, X., Chen, B., Mao, Y., Shao, P., 2023b. Lycopene in hydrophobic deep eutectic solvent with natural catalysts: a promising strategy to simultaneously promote lycopene Z-isomerization and extraction. Food Chem. 426, 136627. https://doi.org/10.1016/j.foodchem.2023.136627.

Zhang, B., Luo, Y., Wang, Q., 2011. Effect of acid and base treatments on structural, rheological, and antioxidant properties of α-zein. Food Chem. 124 (1), 210–220. https://doi.org/10.1016/j.foodchem.2010.06.019.

Zhang, W., Waghmare, P.R., Chen, L., Xu, Z., Mitra, S.K., 2015. Interfacial rheological and wetting properties of deamidated barley proteins. Food Hydrocoll 43, 400–409. https://doi.org/10.1016/j.foodhyd.2014.06.012.

Zhang, W., Zhao, P., Li, J., Wang, X., Hou, J., Jiang, Z., 2022. Effects of ultrasound synergized with microwave on the structure and functional properties of transglutaminase-crosslinked whey protein isolate. Ultrason. Sonochem. 83, 105935. https://doi.org/10.1016/j.ultsonch.2022.105935.

Zhao, Q., Xiong, H., Selomulya, C., Chen, X.D., Huang, S., Ruan, X., Zhou, Q., Sun, W., 2012. Effects of spray drying and freeze drying on the properties of protein isolate from rice dreg protein. Food Bioproc Tech. 6, 1759–1769. https://doi.org/10.1007/s11947-012-0844-3.

Zheng, W.Y., Pang, X.X., Huang, Y.T., Ali, M., Qiu, S.L., Gu, M., Shen, J.L., Lin, Q.y., Zheng, S.X., Liao, L., 2023. Molecular transformation and characterizations of super-deamidated wheat gluten by a tunable hydrated ternary natural deep eutectic solvent. ACS Sustain Chem Eng 11 (19), 7500–7514. https://doi.org/10.1021/acssuschemeng.3c00655.

Zheng, L., Zhao, Y., Xiao, C., Sun-Waterhouse, D., Zhao, M., Su, G., 2015. Mechanism of the discrepancy in the enzymatic hydrolysis efficiency between defatted peanut flour and peanut protein isolate by Flavorzyme. Food Chem. 168, 100–106. https://doi.org/10.1016/j.foodchem.2014.07.037.

Zheng, W.Y., Wu, X.M., Li, M.X., Qiu, S.L., Yang, R., Chen, Z.P., Wang, S.Y., Liao, L., 2022. Synergistic strongly coupled super-deamidation of wheat gluten by glucose-organic acid natural deep eutectic solvent and the efficaciousness of structure and functionality. Food Hydrocoll 125, 107437. https://doi.org/10.1016/j.foodhyd.2021.107437.